

## Fortnightly and monthly variability of the exchange through the Strait of Gibraltar

J.M. Vargas <sup>a,\*</sup>, J. García-Lafuente <sup>a</sup>, J. Candela <sup>b</sup>, A.J. Sánchez <sup>a</sup>

<sup>a</sup> *Departamento de Física Aplicada II, Universidad de Málaga, Málaga, Spain*

<sup>b</sup> *Centro de Investigación Científica y de Educación Superior de Ensenada (CICESE), Ensenada, Baja California, Mexico*

Received 20 December 2004; received in revised form 27 October 2005; accepted 7 July 2006

---

### Abstract

The fortnightly and monthly variability of the exchange through the Strait of Gibraltar has been studied from two simultaneous five-month long moored datasets, at Camarinal Sill and the East Section. The study focuses on the  $M_{sf}$  and  $M_m$  tidal components and their role for the subinertial exchange. A significant monthly signal is observed in the upper layer transport. Also, a significant fortnightly signal is observed in the lower layer transport, which minimum (maximum flow toward the Atlantic) takes place approximately on spring tides. In consequence the net transport has both signals, with maximum taking place during neap tides and a small monthly inequality. Fortnightly and monthly variability in the interface depth is also observed at Camarinal Sill, the interface being deeper on neap and shallower on spring tides. At the East Section the interface depth signals are not significant.

The subinertial variability of the transports is separated in two contributions. The first one is called quasistatic transport and arises from the subinertial fluctuations of currents. The second contribution, called tidally rectified transports, arise from the non-linear correlation of currents and interface depth at tidal frequencies. The tidally rectified transports are important at Camarinal but not at the East Section. An apparent contradiction between the fortnightly signals of the subinertial currents and subinertial transports is resolved when the fortnightly signal of the tidally rectified transports are considered. The fortnightly signal of the quasistatic and tidally rectified transports mutually cancel in the upper layer, but not in the lower layer where the rectified transports dominate. A simple model for the spring-tide mixing forcing accounts for the fortnightly variability of the lower layer quasistatic transports but underestimates it for the upper layer. Finally, the observed lower layer transport is compatible with the hydraulic control condition at Camarinal Sill except for certain periods during intense spring tides.

© 2006 Elsevier Ltd. All rights reserved.

*Keywords:* Strait of Gibraltar; Baroclinic motion; Spring tides; Neap tides; Tidal rectification; Hydraulics

---

---

\* Corresponding author. Address: ETSI Telecomunicación, Campus de Teatinos s/n, Málaga, Spain. Tel.: +34 952133382; fax: +34 952131355.

E-mail address: [jmvargas@ctima.uma.es](mailto:jmvargas@ctima.uma.es) (J.M. Vargas).

### 1. Introduction

#### 1.1. The mean exchange

The Strait of Gibraltar is the only dynamically relevant connection of the Mediterranean Sea with the World Ocean. It is a narrow and shallow channel, with a sill depth of less than 300 m (Camarinal Sill, CS hereinafter) to the west of a narrower region (Tarifa Narrows, TN) of about 15 km of minimum width (Fig. 1a). A small net inflow of fresh water through the Strait is necessary to balance the excess of evaporation minus precipitation over the Mediterranean. Mass and salt conservation force this net inflow to be achieved as a density driven baroclinic flow: fresh ( $S_1 \simeq 36.2$ ) and warm North Atlantic Water flows in at the surface (the upper layer transport,  $Q_1$ ); saltier ( $S_2 \simeq 38.4$ ) and colder Mediterranean Water flows out at depth (the lower layer transport,  $Q_2$ ). Mixing and water entrainment originate an interfacial layer where water properties change gradually. The interfacial layer has a significant thickness and contributes appreciably to the exchanged flows (Bray et al., 1995). However, the inverse-estuarine exchange can still be approximated as a two-layer system of reduced gravity  $g' \simeq 0.02 \text{ m/s}^2$ , mean layer transports  $Q_1 \simeq -Q_2 \simeq 1 \text{ Sv}$ , and mean net transport  $Q_0 = Q_1 + Q_2 < 0.1 \text{ Sv}$ . We will make use of this two-layer system and, in this framework, subindexes 1 and 2 will be used to designate upper and lower layers quantities, respectively.

The amplitude of the transport fluctuations in either layer can be of the same order of magnitude, or higher, than the mean value (Candela et al., 1990; Bryden et al., 1994). Traditionally the fluctuations have been divided into three main frequency bands (Lacombe and Richez, 1982; García-Lafuente and Vargas, 2003):

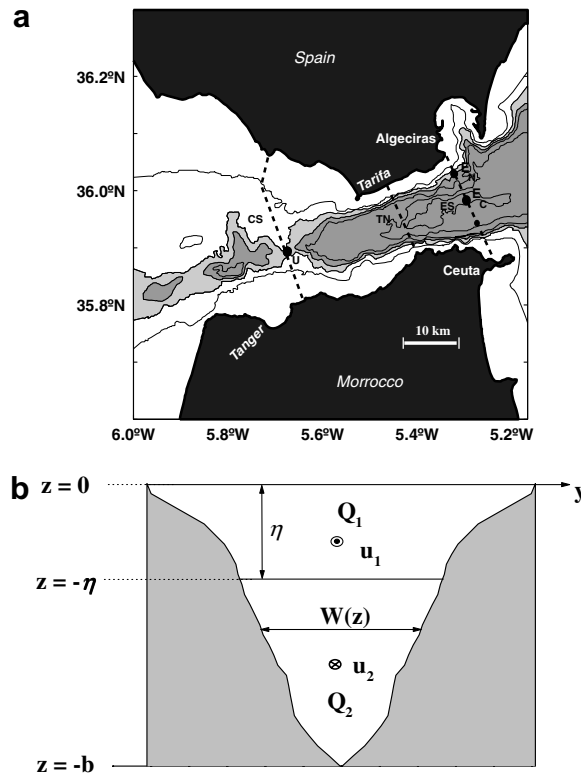


Fig. 1. (a) Bathymetry of the Strait of Gibraltar. Notable sections have been labeled: the main sill (Camarinal Sill, CS), the narrower section (Tarifa Narrows, TN), and the eastern exit (East Section, ES, also called Algeciras–Ceuta section). The mooring sites  $U$ ,  $E_N$  and  $E_C$  are also shown. Isobaths have not been labeled for clarity. Isobaths depths are 100 m, 290 m (to illustrate the depth of Camarinal Sill), 400 m, 500 m, 700 m, and 900 m. Depths greater than 290 m are in light gray, and those greater than 400 m in dark gray. (b) Sketch of a traverse section of arbitrary shape, viewed from the Mediterranean.

tidal, subinertial (periods of some days to several weeks or few months), and low frequency band (seasonal and interannual signals). We will next examine the different contributions to the subinertial band.

### 1.2. Subinertial variability

Three types of fluctuations can be identified within the subinertial band. The first type is known as subinertial barotropic (SBT hereinafter) current fluctuations. The dataset obtained during the *Gibraltar Experiment* (Kinder and Bryden, 1987, 1988) and analyzed by Candela et al. (1989) by means of Empirical Orthogonal Functions (EOF) analysis showed that these barotropic fluctuations account for more than 80% of the subinertial current variance at CS. SBT fluctuations are forced by oscillations of atmospheric pressure over the Mediterranean basin (Crepon, 1965; Candela et al., 1989), and the associated flow fluctuations at the Strait can be quite satisfactorily predicted by numerical models of the atmospheric forcing over the Mediterranean (García-Lafuente et al., 2002a).

The two other types of subinertial fluctuations are related to the complex and energetic tidal dynamics in the Strait. Candela et al. (1990) indicate that, on average, more than 85% of the kinetic energy in the Strait is found within the semidiurnal and diurnal tidal bands. In the vicinity of CS tidal currents are mostly barotropic (Candela et al., 1990), and specially strong (Bruno et al., 1999, 2002), being able to periodically reverse the flow in both layers. During flood, the whole water column may flow westwards, the opposite during ebb (Bryden et al., 1994). This intense tidal forcing has two effects on the subinertial flows: the tidal fortnightly-monthly modulation of the subinertial currents (subinertial baroclinic current fluctuations, SBC) on the one hand, and what will be defined as tidally rectified transports, on the other.

The SBC fluctuations account for approximately 10% of the subinertial current variance at CS. Candela et al. (1989) related them to a second EOF mode of subinertial currents. They did not estimate their associated transports, but they conjectured that its baroclinic character would prevent these fluctuations from contributing to the net transport. The SBC fluctuations may be explained as the modulation of subinertial current shear in areas of tidal mixing like a sill. Hibiya and Leblond (1993) and Hibiya et al. (1998) showed that the effect of fortnightly modulation of the tidal mixing near a sill can be modeled in a simple way assuming a fortnightly modulation of the coefficient of turbulent vertical diffusivity. This is consistent with the fact that the tidally induced turbulence increases mixing on spring tides at CS (Wesson and Gregg, 1994). As a result, the difference between layer-averaged subinertial velocities at CS is enhanced during neap and reduced during spring tides by around 20 cm/s (Candela et al., 1990; Vargas, 2004).

The non-linear interaction of the strong barotropic tidal currents with the bottom topography at CS generates an internal tide of remarkable amplitude (>50 m), which is almost phase-locked with the external tide (La Violette and Lacombe, 1988; La Violette and Arnone, 1988; Bryden et al., 1994). When the net tidal flow points toward the Mediterranean (Atlantic), the interface sinks (shallows) at CS. The tidally rectified transports (also known as *eddy fluxes*, see Bryden et al., 1994) appear as a consequence of the positive correlation between the interface depth and the current fluctuations at tidal frequencies. In order to visualize them, let us consider a simplified two-layer flow with homogeneous layer currents  $u_j$ , and cross-sectional areas  $A_j$  ( $j = 1, 2$ ). With  $\langle \dots \rangle$  we denote a filtering operator that splits those variables into subinertial ( $\langle u_j \rangle$ ,  $\langle A_j \rangle$ ) and tidal ( $\hat{u}_j$ ,  $\hat{A}_j$ , with zero mean) parts:  $u_j = \langle u_j \rangle + \hat{u}_j$  and  $A_j = \langle A_j \rangle + \hat{A}_j$ . In the last expression  $\hat{A}_j$  represents the excess/defect of the instantaneous cross-sectional area over the slowly-varying part  $\langle A_j \rangle$  caused by the vertical fluctuations of the interface at tidal frequencies. The  $j$ th layer transport is computed as

$$Q_j = u_j A_j = \langle u_j \rangle \langle A_j \rangle + \hat{u}_j \hat{A}_j + \langle u_j \rangle \hat{A}_j + \hat{u}_j \langle A_j \rangle. \quad (1)$$

The subinertial transport is obtained by applying the low-pass operator to Eq. (1). It yields:

$$\langle Q_j \rangle = \langle u_j \rangle \langle A_j \rangle + \langle \hat{u}_j \hat{A}_j \rangle, \quad (2)$$

since the average of the product of a subinertial and a zero-mean tidal variable vanishes. Thus, at those sections of the Strait where  $\hat{u}_j$  and  $\hat{A}_j$  are correlated, a non-linear tidal contribution  $\langle \hat{u}_j \hat{A}_j \rangle$  to the subinertial transport arises. This contribution will be named tidally rectified (TR) transport.

The first term of the right hand side (rhs) in Eq. (2) will be called quasistatic (QS) transport, and will be more precisely defined in Section 3.4. It accounts for the contribution of the long-term current, plus the SBT and SBC fluctuations. The TR transport contributes not only to the subinertial variability but also to the long-term mean of the transports. Both terms together form the subinertial transports  $\langle Q_j \rangle$ .

The TR transports are an aspect of the baroclinic character of the tide in the Strait. Therefore, they must be of considerable importance in the vicinity of CS, the main topographic obstacle of the Strait (Fig. 1a). The amplitude of the baroclinic or internal tide decreases with distance as it radiates out from CS. Accordingly, the importance of the TR transports also diminishes. In fact, their magnitude at CS has been estimated in the range 0.3–0.4 Sv (Bryden et al., 1994; Tsimplis and Bryden, 2000), whereas at the East Section (ES, hereinafter) they are an order of magnitude smaller (García-Lafuente et al., 2000).

### 1.3. Fortnightly and monthly tidal signals

The reported values for fortnightly ( $M_{sf}$ ) and monthly ( $M_m$ ) signals of the transports are relatively scarce, fractional and somewhat contradictory (see Table 1). Thus, it is not possible to give precise values for their amplitudes and phases. Bryden et al. (1994) found a fortnightly signal of around 0.1 Sv for both upper and lower layers at CS, with minimum upper and lower layer transports taking place two or three days after spring tides. The estimates by García-Lafuente et al. (2000) at ES are in reasonable agreement with the former for the fortnightly amplitudes, but they provide smaller phases that point to minimum upper and lower layer transports on spring tides (Table 1). Tsimplis and Bryden (2000) estimated an unrealistically high amplitude of 0.46 Sv for the fortnightly signal of the upper layer transport at CS. Bryden et al. (1994) reported a small fortnightly signal (0.03 Sv) for the net transport. A fortnightly amplitude of the net transport as high as 0.20 Sv has been reported at ES by García-Lafuente et al. (2002b). Only Tsimplis and Bryden (2000) and García-Lafuente et al. (2000) provide constants for the monthly signal of the exchanged transports. Both found a monthly amplitude of the upper layer transport of 0.15 Sv, greater than for the lower layer transport (0.05 Sv), but estimated very different phases.

The fortnightly signal of the interface depth at CS is about 20 m in amplitude, deeper on neap tides, shallower on spring tides (Bryden et al., 1994; Tsimplis and Bryden, 2000). The interface cross-slope at CS is steeper around neap tides, consistent with the increase of the subinertial currents shear during neap tides (Candela et al., 1989).

Given the tidal and intrinsically non-linear origin of the TR transports, they must reasonably have certain fortnightly and monthly variability. However, there is no information on this issue, even when the important contribution of the TR transports to the mean exchange has been already recognized (Bryden et al., 1994).

Table 1

Previously available fortnightly constants (amplitude  $A_{M_{sf}}$  and phase  $\phi_{M_{sf}}$ ), and monthly constants (amplitude  $A_{M_m}$  and phase  $\phi_{M_m}$ ) for the upper layer ( $Q_1$ ), lower layer ( $Q_2$ ) and net ( $Q_0$ ) transports

	$A_{M_m}$ (Sv)	$\phi_{M_m}$ (°)	$A_{M_{sf}}$ (Sv)	$\phi_{M_{sf}}$ (°)
<i>Bryden et al. (1994), Camarinal Sill</i>				
$Q_1$	n/a	n/a	$0.10 \pm 0.10$	$255 \pm 40$
$Q_2$	n/a	n/a	$0.10 \pm 0.10$	$230 \pm 35$
<i>Tsimplis and Bryden (2000), Camarinal Sill</i>				
$Q_1$	0.15	225	0.46	210
$Q_2$	0.05	25	0.15	50
<i>García-Lafuente et al. (2000), East Section</i>				
$Q_1$	0.15	110	0.10	185
$Q_2$	0.05	75	0.10	195
$Q_0$	0.20	100	0.15	185
<i>García-Lafuente et al. (2002a), East Section</i>				
$Q_0$	n/a	n/a	$0.20 \pm 0.10$	$140 \pm 20$

n/a stands for non-available.

#### 1.4. Hydraulics

The Strait of Gibraltar is a relatively well known example of a strait where the exchange is suitably described in the frame of the two-layer hydraulic approximation (Hogg et al., 2001). Basically, this is equivalent to stating that, given the density difference between the basins and the value of the net evaporation over the Mediterranean, the Strait topography is the main factor determining the exchanged flows. A key concept in this framework is the control section (Bryden and Stommel, 1984; Armi and Farmer, 1986): the flow is controlled in certain singular sections where the composite Froude number  $G^2$  equals one:

$$G^2 = F_1^2 + F_2^2 = 1. \quad (3)$$

In this equation,  $F_j^2$  is the internal Froude number of the  $j$ th layer which can be expressed as (see, for example, Delgado et al., 2001):

$$F_j^2 = \frac{Q_j^2 W_{\text{int}}}{g' A_j^3}, \quad (4)$$

where  $W_{\text{int}}$  is the sectional width at the depth of the interface and  $g'$  is the reduced gravity. In the steady hydraulic theory the control condition is achieved at topographic singular sections or in their vicinity (Armi and Farmer, 1986; Farmer and Armi, 1986). As CS is the minimal area section of the Strait of Gibraltar, it has historically been regarded as its main control section (Bryden and Stommel, 1984; Bormans and Garrett, 1989). In the framework of the steady theory, it is also usually assumed that the composite Froude number at CS is dominated by the lower layer Froude number, that is  $F_1^2 \ll F_2^2$ , so that the control condition at CS may be written as  $F_2^2 \simeq 1$ . Presently it is accepted, however, that the control at CS is periodically lost during certain parts of the tidal cycle particularly during spring tides (Armi and Farmer, 1988). Two layer numerical tidal models of the exchange (e.g., Castro et al., 2004) provide the same result.

#### 1.5. Paper organization

In this paper we provide new information on the fortnightly and monthly variability of the exchanged transports, as well as the contribution of the different types of fluctuations to these signals. The paper is organized as follows: in Section 2 we present the dataset and explain the method followed in the determination of the interface depth and transports, which is based on that shown in García-Lafuente et al. (2000). In Section 3 we analyze the monthly and fortnightly variability of the exchange through the Strait of Gibraltar. The EOF decomposition of subinertial currents is carried out in Section 3.1 with the objective of providing a compact representation for the fortnightly and monthly signals of the subinertial velocity field, and of identifying its barotropic and baroclinic fluctuations. Fortnightly and monthly variability of the net and exchanged transports is analyzed in Section 3.3. A method to split the subinertial exchanged transports into the contributions indicated in Eq. (2) is explained in Section 3.4, and once the contributions have been separated, we analyze the fortnightly and monthly signals in quasistatic and tidally rectified transports in 3.5 and its compensation in Section 3.6. The harmonic constants of these contributions help to understand the behavior of the exchanged transports at these frequencies. In Section 3.7 we explore the relation between the tidal mixing forcing and the SBC fluctuations, while in Section 3.8 we analyze the implications of our results for the hydraulic control at the Strait. Finally, in Section 4 we summarize the most interesting results of this paper.

## 2. Data and methodology

### 2.1. Data

The dataset consists of velocity and salinity data obtained simultaneously at CS and ES. At CS two moorings were deployed close to each other (position  $U$  in Fig. 1a). The first one was a short ( $\simeq 10$  m) mooring equipped with an upper-looking Acoustic Doppler Current Profiler (ADCP) that measured the vertical current profile, from near the bottom to near the surface, with 8 m vertical bins and 15 min sampling interval. The

Table 2

Deployment information of the moorings: start and end dates, nominal depth of the instruments and bottom depth

Mooring	Start	End	Nominal depths (m)	Bottom depth (m)
N	10/24/95	05/08/96	30, 60, 120, 250, 410	450
C	10/17/95	04/18/96	30, 55, 75, 110, 160, 265, 765	920
U	10/16/95	04/20/96	44 ↔ 276 (8 m bins)	280
U'	10/16/95	03/19/96	75, 145, 175, 225	280

Moorings N and C are located at ES while mooring U and U' are at CS.

second mooring, aimed to monitor the time evolution of the depth of the interface, had a subsurface float at a depth of 60 m and four instruments: two Aanderaa RCM-7 currentmeters equipped with temperature, salinity and depth sensors, sampling every hour, and two Seabird Seacats measuring temperature, salinity and depth every 10 minutes. All time series were smoothed and resampled to hourly values for further processing. At ES two mooring locations were occupied with Aanderaa RCM-7 currentmeters also equipped with pressure, temperature and conductivity sensors. Northern and Central moorings are denoted as  $E_N$  and  $E_C$  in Fig. 1a. Table 2 summarizes the deployment information. The simultaneous time series are 147 days long, beginning on October 24, 1995 and ending on March 19, 1996.

The present work is primarily concerned with the subinertial variability of the data and, in particular, of the exchanged transports. We work with the along-strait currents  $u_\alpha$ , where  $\alpha = 15^\circ$  counterclockwise from the east direction is the angle that defines the along-strait direction. The low-pass operator  $\langle \cdot \cdot \cdot \rangle$  used to obtain the subinertial series is implemented with a 8<sup>th</sup> order low-pass Butterworth filter with pass-band and stop-band frequencies  $f_1 = 0.0263$  cph (38 h) and  $f_2 = 0.0357$  cph (28 h), respectively. Fig. 2 shows the time series of the  $u_{15}$  subinertial currents at CS, along with the tidal elevation at Tarifa harbour (this plot is repeatedly used as a “clock” in subsequent figures to highlight the strength and timing of spring and neap tides). A certain monthly and fortnightly variability can be observed, with stronger inflowing currents in the upper layer and outflowing current in the lower layer on spring tides. Notice that during strong spring tides subinertial currents may point westward in the whole water column.

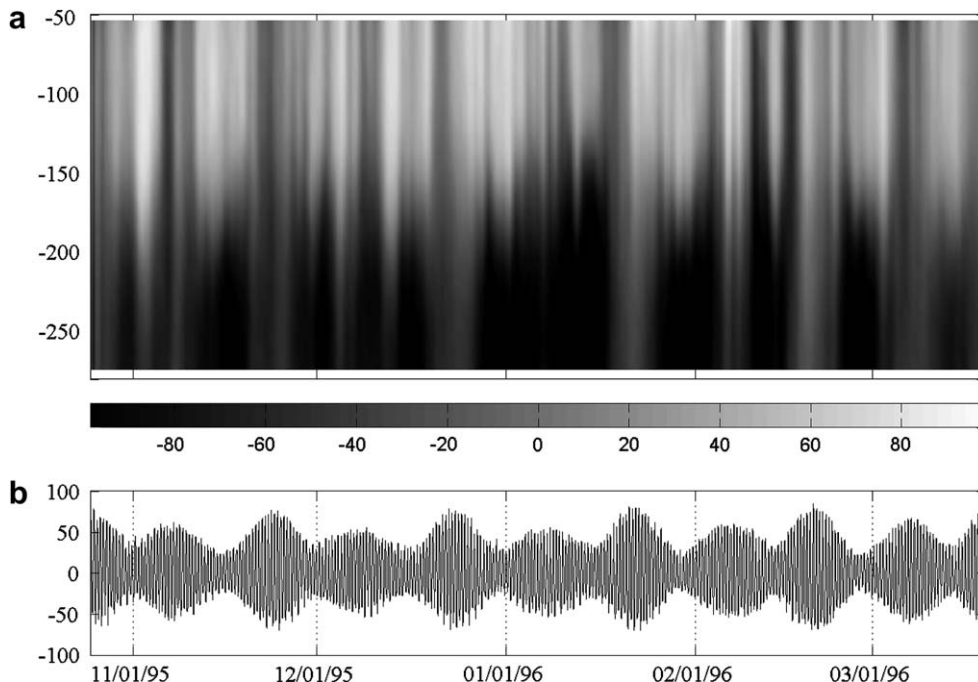


Fig. 2. (a) Depth–time contours of the along strait subinertial currents,  $\langle u_{15} \rangle$  (cm/s) at CS. (b) Tidal signal of the sea level at Tarifa.

## 2.2. Flow definitions and estimations

The data at ES are a subset of the data used by García-Lafuente et al. (2000) to study the tidal variability in this section, and the methodology is almost the same than in that paper. In particular, the salinity drift corrections, the division of the section into three subareas, the linear extrapolation of the central current profiles to the southern subarea, the transports definitions and estimation procedure (with the only exception of interface depth estimation, a question that is addressed in next section) in the present work, are the same as in García-Lafuente et al. (2000). The reader is referred to this paper for further details.

Transport estimates at CS have been obtained using the following simplified equations:

$$Q_1(t) = \int_{z=-\eta(t)}^{z=0} u_x(z, t) W_{CS}(z) dz, \quad (5)$$

$$Q_2(t) = \int_{z=-b}^{z=-\eta(t)} u_x(z, t) W_{CS}(z) dz, \quad (6)$$

where  $u_x(z, t)$  is the along-strait current profile,  $W_{CS}(z)$  the width of the Strait at depth  $z$  and  $\eta(t)$  is the interface depth (see the sketch of Fig. 1b). Velocity data were linearly interpolated. The width function  $W_{CS}$  and the procedure for velocity data extrapolation to the surface are the same as in Bryden et al. (1994).

## 2.3. Determination of the interface depth

A common procedure to define the depth of the interface is the choice of a material surface of a given salinity. For example, Bryden et al. (1994) used  $S = 37$  at CS, while García-Lafuente et al. (2000) used  $S = 37.9$  at ES. In both cases some property of the flow was invoked and the salinity of the interface was constant by definition.

Here a slightly more sophisticated method has been followed. First, we define an interfacial region bounded by two isohaline surfaces  $S_l$  and  $S_u$  at its lower and upper limits, respectively, with  $S_u < S_l$ . At CS where the mean salinity of the interface must not differ too much from the value  $S = 37.0$  suggested by Bryden et al. (1994), we use  $S_u = 36.6$  and  $S_l = 38.0$ . At ES, where García-Lafuente et al. (2000) suggested  $S = 37.9$ , we use  $S_u = 37.0$  and  $S_l = 38.4$ .

Once defined this interfacial region, we select different isohalines  $S$  within this range and use their depths  $z_S(t)$  instead of  $\eta(t)$  in Eqs. (5) and (6) to compute the associated transports  $Q_{1S}$  and  $Q_{2S}$ . In practice, we compute them at salinity steps of 0.1. For each instant  $t$ , the interface depth  $\eta(t)$  is obtained as the depth of the isohaline that maximizes the difference  $Q_{1S}(t) - Q_{2S}(t)$ . Note that this difference is not the net flow, which is given by  $Q_{1S} + Q_{2S}$ . Mathematically, the maximization conditions are

$$\frac{\partial}{\partial S} [Q_{1S}(t) - Q_{2S}(t)]_t = 0, \quad (7)$$

$$\frac{\partial^2}{\partial S^2} [Q_{1S}(t) - Q_{2S}(t)]_t < 0. \quad (8)$$

To carry out the former computations we need to know the depth of isohaline  $S$ . This depth is computed from salinity observations at the mooring locations. Linear interpolation of salinity profiles have been previously used (Bray et al., 1995; García-Lafuente et al., 2000), but here we apply an improved procedure. A sigmoidal function of the form (see also Echevarria et al., 2002)

$$S(z, t) = \frac{s_2(t) - s_1(t)}{\left[1 + \exp\left(\frac{z - z_0(t)}{\Delta z(t)}\right)\right]} + s_1(t), \quad (9)$$

where the depth  $z$  is positive upwards and  $z = 0$  is the sea surface, is used for the interpolation.  $z_0(t)$ ,  $\Delta z(t)$ ,  $s_1(t)$ ,  $s_2(t)$  are fitting parameters to be estimated. The parameter  $z_0$  represents the depth of the midpoint of the halocline, while  $\Delta z(t)$  is a (positively defined) measure of the halocline thickness  $\delta z$ , which can be approximated by  $\delta z \simeq 6\Delta z$ . The salinity at the surface approaches  $s_1$  while salinity near the bottom coincides with  $s_2$ ,

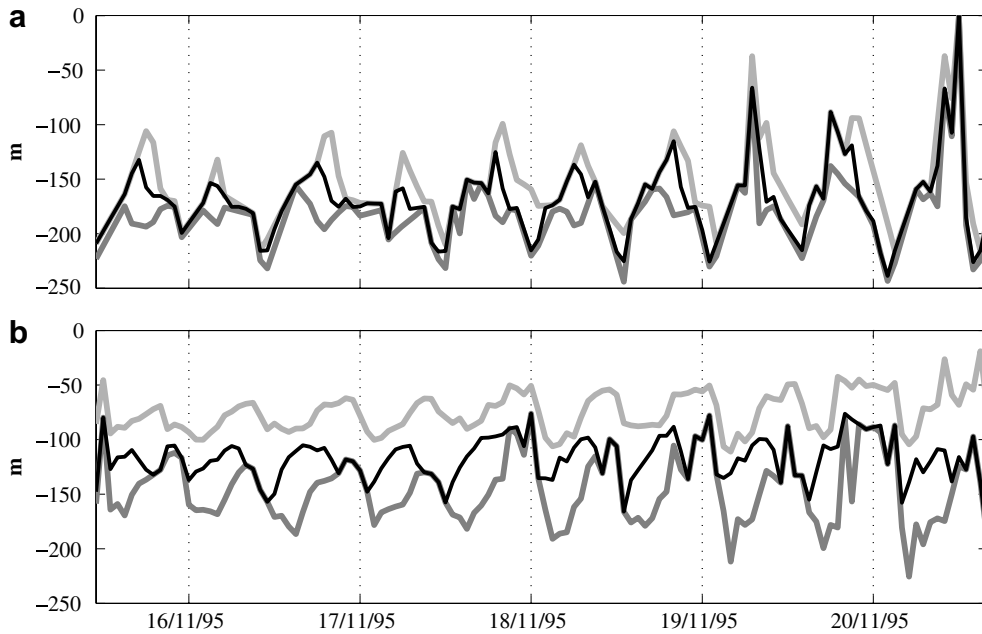


Fig. 3. Depth of the isohalines  $S_u$  (light gray) and  $S_l$  (dark gray), along with the estimated interface depth  $\eta$  (black), for a short period in November 1995, at (a) CS and (b) ES.

provided the bottom is much deeper than the lower part of the halocline, located at  $z \simeq z_0 - 3\Delta z$ . Because these last conditions are usually met, bottom salinity practically equals  $s_2$ . Besides, the lower layer salinity is fairly constant so that  $s_2$  has been fixed to  $s_2(t) = 38.4$ , which is the salinity of the Mediterranean outflow. This physical argument reduces the number of free parameters to three. The three other fitting parameters have been estimated from the salinity data acquired by the currentmeters. Once evaluated, the inversion of Eq. (9) provides the interpolated depth  $z_S(t)$  of any isohaline  $S$ . Fig. 3 shows the time series of  $z_{Su}$ ,  $z_{Sl}$ , and  $\eta$  at both ES and CS for a five days period. It can be seen how the interface moves within the depth range of the limiting isohalines during the tidal cycle. The exchanged transports are then estimated from  $\eta(t)$ .

### 3. Results

#### 3.1. Subinertial currents fluctuations

To investigate the subinertial variability of currents we performed an EOF decomposition of the  $u_{15}$  subinertial currents. The first and second EOF modes explain more than 90% of the variance of the subinertial currents at both sections ((60 + 36)% at CS, (85 + 12)% at ES). Their spatial patterns (panels (b) and (c) of Fig. 4) correspond clearly to barotropic and baroclinic modes, respectively, so that they will be denoted as SBT and SBC modes. The spatial patterns and temporal variability (panels (d) and (e) of Fig. 4) of this modes have similar characteristics to those described by Candela et al. (1989).

Panel (f) of Fig. 4 shows the time series of subinertial  $u_{15}$  fluctuations associated with the SBC mode at CS. Their fortnightly and monthly variability is more evident than that of the pure subinertial  $u_{15}$  currents (Fig. 2) because the meteorologically forced signal is now included in the SBT fluctuations. A harmonic analysis of the dimensionless time coefficient series  $\Psi_{SBT}$  and  $\Psi_{SBC}$  (Table 3) confirms this conclusion: fortnightly and monthly signals are not significant in the SBT mode, but they are in the SBC mode. For the latter, they combine to produce positive values of the temporal coefficients on neap tides, negative on spring tides, and a certain monthly inequality. The size of velocity fluctuations at these frequencies are obtained by multiplying the SBC mode vertical profile (Fig. 4b, gray line) by the corresponding amplitudes of its time coefficient series shown in Table 3. The fortnightly signal is around 15 cm/s at  $z \simeq 100$  m (upper layer) and around  $-20$  cm/s at  $z \simeq 220$  m (lower

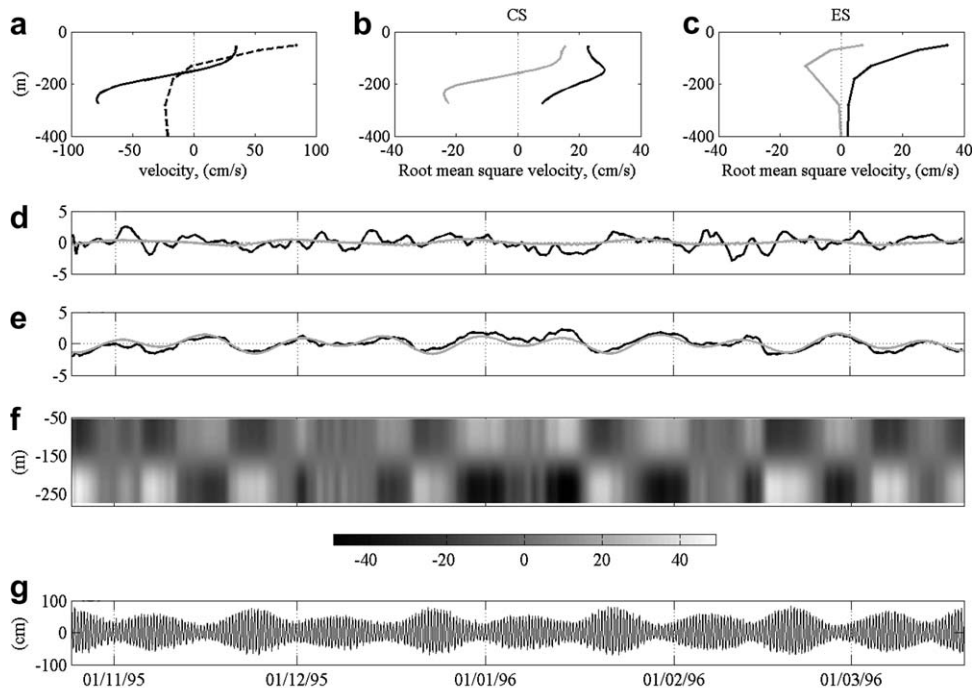


Fig. 4. (a) Long term mean velocity profiles at CS (solid line) and ES (dashed). Vertical profiles of rms velocity of subinertial currents SBT (black) and SBC (gray) modes at (b) CS and (c) ES. Non-dimensional time coefficient series of (d) SBT mode  $\Psi_{\text{SBT}}$ , and (e) SBC mode  $\Psi_{\text{SBC}}$  (black), along with their  $M_m + M_{\text{sf}}$  harmonic fit (gray), at CS. (f) Depth-time contour plot of SBC current fluctuations at CS (cm/s) (g) Tidal signal of the sea level at Tarifa.

layer), both peaking one day after neap tides ( $\phi_{M_{\text{sf}}} = 210^\circ$ ). These fluctuations modify the mean current profiles (Fig. 4a), giving maximum subinertial shear on neap tides and minimum on spring tides, in agreement with the conclusion by Candela et al. (1989). Fortnightly currents have a similar pattern at ES but their amplitudes are approximately half the amplitudes at CS. At both sections the computed monthly signal is smaller than the fortnightly signal, but still significant.

This EOF decomposition of the velocity field will be used later to explain some properties of the estimated transports.

### 3.2. Estimated transports

The transports estimated according to the methodology described in Section 2.2 are compatible with previously reported estimations, the only exception being the upper layer transport at CS. Due to the uncertainty in the effective size of the upper layer cross-section and in the near surface extrapolated ADCP velocities at CS, we have obtained an unrealistic high value of the mean upper layer transport, significantly larger than both the mean upper layer transport at ES and the mean lower layer transport at CS. The first circumstance violates volume conservation in the upper layer, while the second one overestimates the net evaporative rate of the Mediterranean Sea. For these physical reasons, the upper layer transport at CS has to be reduced by a factor  $R$ . This factor has been estimated by imposing that the difference of the net transports estimated at both sections had zero mean and minimum variance (as a function of  $R$ ). A compromise for these two conditions is found when the initially estimated upper layer transport at CS is reduced by a factor  $R \simeq 0.85$ . With this correction, the long term mean of the estimated exchanged transports are  $\bar{Q}_1 \simeq 0.9$  Sv and  $\bar{Q}_2 \simeq 0.8$  Sv at both sections. These are similar values to other previously reported (Bryden et al., 1994; García-Lafuente et al., 2000, 2002b; Tsimplis and Bryden, 2000; Candela, 2001). It should be noted that the present are the first reported simultaneous estimates of the exchange at two different sections during a time period as long as five months.

Table 3

Mean value, standard deviation (total/subinertial), and harmonic constants of  $M_m$  and  $M_{sf}$  constituents for the dimensionless temporal series of the SBT and SBC modes ( $\Psi_{SBT}$ ,  $\Psi_{SBC}$ ), upper layer transport ( $Q_1$ ), lower layer transport ( $Q_2$ ), net transport ( $Q_0$ ), quasistatic transports ( $Q_1^{QS}$ ,  $Q_2^{QS}$ ) and tidally rectified transports ( $Q_1^{TR}$ ,  $Q_2^{TR}$ ), interface depth ( $\eta$ ), and reduced gravity  $g'$  at both sections, and along strait interface slope  $\Delta\eta = \eta(\text{ES}) - \eta(\text{CS})$  (n.a. stands for not applicable)

	Mean	Std	$A_{M_m}$	$\phi_{M_m}$	$A_{M_{sf}}$	$\phi_{M_{sf}}$
$\Psi_{SBT}$	0	1/1	$0.4 \pm 0.4$	$90 \pm 55$	$0.1 \pm 0.4$	$150 \pm 160$
$\Psi_{SBC}$	0	1/1	$0.6 \pm 0.3$	$185 \pm 25$	$1.0 \pm 0.3$	$210 \pm 20$
$Q_1(\text{CS})$	0.9	1.7/0.4	$0.20 \pm 0.10$	$90 \pm 40$	$0.10 \pm 0.10$	$100 \pm 90$
$Q_1(\text{ES})$	0.9	0.6/0.4	$0.20 \pm 0.10$	$90 \pm 30$	$0.10 \pm 0.10$	$140 \pm 70$
$Q_2(\text{CS})$	-0.8	1.3/0.4	$0.15 \pm 0.10$	$160 \pm 40$	$0.25 \pm 0.10$	$200 \pm 20$
$Q_2(\text{ES})$	-0.8	2.6/0.6	$0.10 \pm 0.10$	$100 \pm 70$	$0.20 \pm 0.15$	$200 \pm 40$
$Q_0(\text{CS})$	0.1	2.7/0.7	$0.30 \pm 0.20$	$120 \pm 40$	$0.25 \pm 0.20$	$180 \pm 50$
$Q_0(\text{ES})$	0.1	2.7/0.6	$0.30 \pm 0.20$	$90 \pm 40$	$0.25 \pm 0.20$	$180 \pm 50$
$Q_1^{QS}(\text{CS})$	0.6	0.5/0.5	$0.20 \pm 0.15$	$135 \pm 40$	$0.25 \pm 0.15$	$190 \pm 40$
$Q_2^{QS}(\text{CS})$	-0.4	0.4/0.4	$0.10 \pm 0.10$	$60 \pm 50$	$0.10 \pm 0.10$	$60 \pm 50$
$Q_1^{QS}(\text{ES})$	>0.8	0.4/0.4	$0.15 \pm 0.10$	$90 \pm 30$	$0.10 \pm 0.10$	$135 \pm 70$
$Q_2^{QS}(\text{ES})$	<-0.7	0.4/0.4	$0.10 \pm 0.15$	$100 \pm 70$	$0.20 \pm 0.15$	$200 \pm 40$
$Q_1^{TR}(\text{CS})$	0.3	0.3/0.3	$0.15 \pm 0.05$	$10 \pm 10$	$0.30 \pm 0.05$	$30 \pm 10$
$Q_2^{TR}(\text{CS})$	-0.4	-0.4/ - 0.4	$0.20 \pm 0.05$	$190 \pm 10$	$0.35 \pm 0.05$	$210 \pm 10$
$Q_1^{TR}(\text{ES})$	<0.1(in absolute value)			n.a.	n.a.	n.a.
$Q_2^{TR}(\text{ES})$	<0.1(in absolute value)			n.a.	n.a.	n.a.
$\eta(\text{CS})$	155	60/25	$10 \pm 10$	$170 \pm 40$	$25 \pm 10$	$200 \pm 20$
$\eta(\text{ES})$	120	40/20	$5 \pm 10$	$60 \pm 100$	$10 \pm 10$	$70 \pm 60$
$\Delta\eta$	35	55/30	$15 \pm 5$	$190 \pm 20$	$29 \pm 5$	$215 \pm 10$
$g'(\text{CS})$	0.018		$0.0010 \pm 0.0001$	$180 \pm 50$	$0.001 \pm 0.0001$	$210 \pm 40$
$g'(\text{ES})$	0.015		$0.0015 \pm 0.0001$	$195 \pm 80$	$0.003 \pm 0.001$	$230 \pm 35$

Panels (a) in Fig. 5 show the computed net transports at both sections. They are dominated by tidal variability and are quite similar. Ideally they should be identical, therefore their differences must be attributed to sampling and estimation errors. The estimated subinertial standard deviation, 0.6–0.7 Sv, is higher than the estimation of 0.4 Sv of Candela et al. (1989).

At tidal frequencies the time series of upper and lower layer transports differ considerably from one section to the other (compare left and right plots of panels (b) and (c) in Fig. 5). This indicates strong internal divergences, a dynamical feature that has been previously reported by Candela et al. (1990) and García-Lafuente et al. (2000). In contrast, their subinertial time series are very similar (Fig. 6), with a correlation coefficient of  $r_1 \simeq 0.9$  for the upper layer, and  $r_2 \simeq 0.7$  for the lower layer.

### 3.3. Fortnightly and monthly signals

Table 3 shows the results of the harmonic analysis of the subinertial time series of the net transport ( $\langle Q_0 \rangle$ ), exchanged transports ( $\langle Q_1 \rangle$  and  $\langle Q_2 \rangle$ ), and interface depth ( $\langle \eta \rangle$ ) for  $M_{sf}$  and  $M_m$  constituents. Although errors are high both in amplitude and phase, the independent estimations for each constituent carried out on each section are similar, which gives confidence to our transport calculations.

The monthly signal of the upper layer transport has a significant amplitude of around 0.2 Sv, but the upper layer transport fortnightly variability is not significant, as the fortnightly amplitude is the same as its estimated error (0.1 Sv). This result agrees with those by Bryden et al. (1994) and García-Lafuente et al. (2000), and also agrees with the lack of evidence of fortnightly signals of the sea level in the analysis by Garrett et al. (1989). However, it clearly disagrees with the  $M_{sf}$  amplitude of 0.46 Sv estimated at CS for the upper layer transport by Tsimplis and Bryden (2000).

The fortnightly constituent  $M_{sf}$  of the lower layer transport has a significant amplitude of 0.25 Sv at CS and 0.20 Sv at ES, suggesting the existence of a deterministic signal. The maximum lower layer transport, minimum flow toward the Atlantic, takes place during neap tides. The monthly constituent has less significant

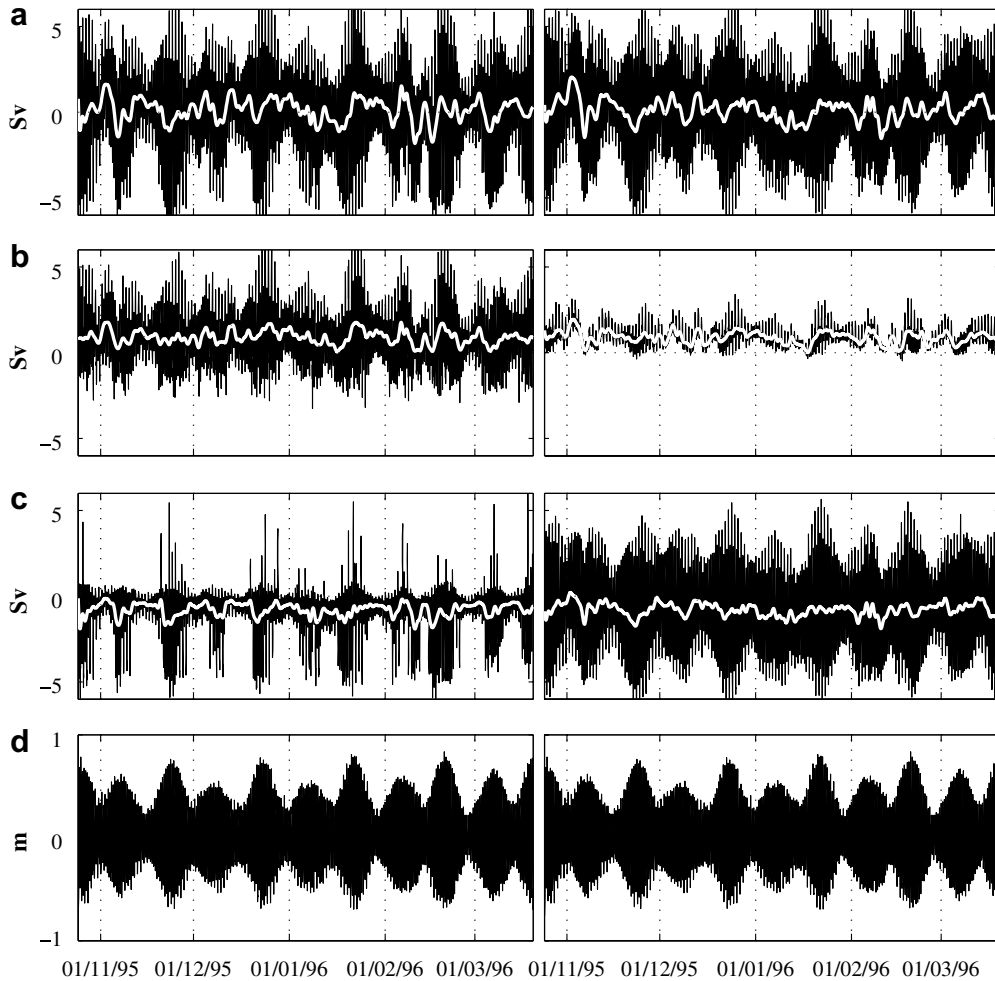


Fig. 5. Estimated instantaneous (black) and subinertial transports (white) at CS (left panels) and ES (right panels): (a) Net transport  $Q_0$ , (b) upper layer transport  $Q_1$ , (c) lower layer transport  $Q_2$ . (d) Tidal signal of the sea level at Tarifa.

amplitudes of  $(0.15 \pm 10)$  Sv at CS and  $(0.10 \pm 0.10)$  Sv at ES. Thus, the time series of the subinertial lower layer transport essentially shows fortnightly variability (Fig. 6a).

Consequently, the net transport has both fortnightly and monthly constituents with significant amplitudes ( $0.25$  Sv and  $0.30$  Sv, respectively). The phase of the fortnightly constituent ( $180^\circ$ ) is such that the maximum of the net transport takes place on neap tides, coinciding with the above mentioned maximum of the lower layer transport. This agrees with García-Lafuente et al. (2002a), who found a fortnightly signal of similar amplitude and phase in a period of five months between October of 1997 and March of 1998.

There is some apparent contradiction between the harmonic constants of subinertial transports in Table 3 and those obtained through EOF analysis in Section 3.1 for the subinertial currents at CS. The phase of the fortnightly signal of the lower layer transport ( $200^\circ$ ) is nearly opposite to that of the lower layer subinertial currents ( $30^\circ$ ). Also, the monthly signal for the upper layer transport is in quadrature with the upper layer subinertial currents. These apparent contradictions disappear when TR transports are taken into account, as we will show in Section 3.6.

At CS the interface depth shows a dominant fortnightly variability with an amplitude of  $25$  m, and a phase such that the minimum depth is achieved less than one day after spring tide. On the contrary the interface depth at ES has no significant fortnightly variability. Consequently, the fortnightly variability of the difference  $\Delta\eta = \eta(\text{ES}) - \eta(\text{CS})$ , the along-strait interface slope, has noticeable amplitudes (Table 3). Its phase is such that

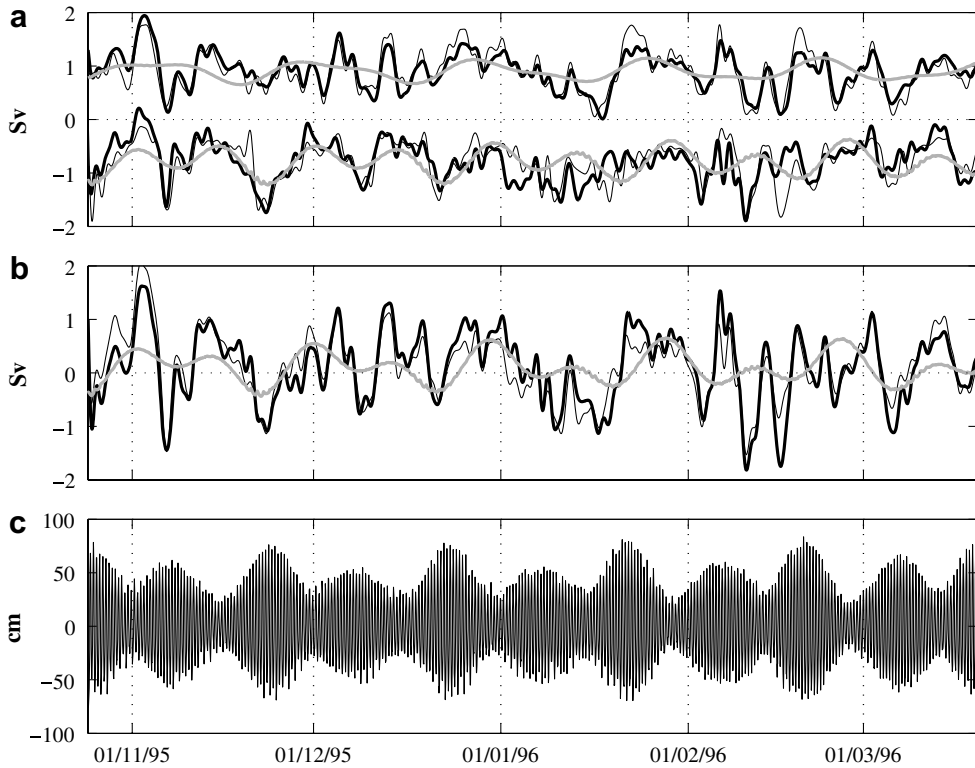


Fig. 6. Subinertial time series of the estimated transports at CS (black, thick line) and ES (black, thin line), and  $M_m + M_{sr}$  harmonic fit (gray line) of the CS time series: (a) Subinertial upper layer and lower layer transports,  $\langle Q_1 \rangle$ ,  $\langle Q_2 \rangle$ . (b) Subinertial net transport  $\langle Q_0 \rangle$ . (c) Tidal signal of the sea level at Tarifa.

the maximum slope takes place a day after spring tides. The monthly signal is not significant for the interface fluctuations at any section but, curiously, it is for  $\Delta\eta$ . A possible explanation is that the interface difference tends to cancel out the meteorologically-induced noise that is present in the subinertial band. The noise contributes to the error estimates when analyzing data of each section separately, but disappears in the interface difference  $\Delta\eta$  because it is coherent for spatial scales larger than the dimension of the Strait.

### 3.4. Tidally rectified and quasistatic transports

In the so called quasistatic approximation the acceleration term in the equations of motion is neglected for subinertial and lower frequency motions and the velocity fluctuations at these time scales are modeled as a slow evolution between steady states. At tidal frequencies the quasistatic approximation fails (Helfrich, 1995). Thus, although the TR transports are subinertial, they are non-quasistatic as they do not arise from subinertial currents, but from non-linear interactions between currents and interface depth fluctuations at tidal frequencies. In contrast, subinertial current fluctuations give rise to quasistatic (QS) transports, than can be separated into SBT and SBC parts. Despite the fact that SBC currents are indirectly forced through tidal mixing, their associated transports are quasistatic, as they arise from subinertial current variability. This section deals with these two types of transports, quasistatic (QS) and tidally rectified (TR). In order to compute them we must derive an extended version of Eq. (2). Let us split the measured time series of currents  $u_x(z,t)$  and the derived time series of the interface depth  $\eta(t)$  at a given section into subinertial and tidal parts in the way explained in Section 1:

$$u_x(z,t) = \langle u_x(z,t) \rangle + \hat{u}_x(z,t), \tag{10}$$

$$\eta(t) = \langle \eta(t) \rangle + \hat{\eta}(t), \tag{11}$$

where as in Section 1,  $\langle \dots \rangle$  denote subinertial part and  $(\widehat{\dots})$  zero mean tidal part. The QS parts of the transports are obtained from the subinertial currents and interface depth. More explicitly:

$$Q_1^{QS} = \int_{z=-\langle \eta \rangle}^{z=0} \langle u_z \rangle W dz, \tag{12}$$

$$Q_2^{QS} = \int_{z=-b}^{z=-\langle \eta \rangle} \langle u_z \rangle W dz. \tag{13}$$

Using Eqs. (5) and (6) and the decompositions (10) and (11), the total instantaneous transports can be written as

$$Q_1 = \int_{z=-\eta}^{z=-\langle \eta \rangle} \langle u_z \rangle W dz + \int_{z=-\langle \eta \rangle}^{z=0} \langle u_z \rangle W dz + \int_{z=-\eta}^{z=-\langle \eta \rangle} \widehat{u}_z W dz + \int_{z=-\langle \eta \rangle}^{z=0} \widehat{u}_z W dz, \tag{14}$$

$$Q_2 = \int_{z=-b}^{z=-\langle \eta \rangle} \langle u_z \rangle W dz + \int_{z=-\langle \eta \rangle}^{z=-\eta} \langle u_z \rangle W dz + \int_{z=-b}^{z=-\langle \eta \rangle} \widehat{u}_z W dz + \int_{z=-\langle \eta \rangle}^{z=-\eta} \widehat{u}_z W dz, \tag{15}$$

which are elaborated versions of Eq. (1). The first and third terms of the rhs of Eq. (14) account for the fluctuating part of the interface due to tidal motions, that is, they are the counterpart of  $\widehat{A}_1$  in Eq. (1). The same holds for the second and fourth terms of the rhs of Eq. (15) and  $\widehat{A}_2$  in Eq. (1).

Applying the low-pass operator to obtain the subinertial transports  $\langle Q_1 \rangle$  and  $\langle Q_2 \rangle$  we have

$$\langle Q_1 \rangle = \left\langle \int_{z=-\eta}^{z=-\langle \eta \rangle} \langle u_z \rangle W dz \right\rangle + Q_1^{QS} + \overbrace{\left\langle \int_{z=-\eta}^{z=-\langle \eta \rangle} \widehat{u}_z W dz \right\rangle}^{Q_1^{TR}} + \left\langle \int_{z=-\langle \eta \rangle}^{z=0} \widehat{u}_z W dz \right\rangle, \tag{16}$$

$$\langle Q_2 \rangle = Q_2^{QS} + \left\langle \int_{z=-\eta}^{z=-\langle \eta \rangle} \langle u_z \rangle W dz \right\rangle + \underbrace{\left\langle \int_{z=-\langle \eta \rangle}^{z=-\eta} \widehat{u}_z W dz \right\rangle}_{Q_2^{TR}} + \left\langle \int_{z=-b}^{z=-\langle \eta \rangle} \widehat{u}_z W dz \right\rangle, \tag{17}$$

where the definitions (12) and (13) have been used. The first and fourth terms of the rhs in (16) and the second and fourth terms of the rhs in (17) are equivalent to the terms  $\langle u_j \rangle \widehat{A}_j$  and  $\widehat{u}_j \langle A_j \rangle$  in (1), respectively, and their time average is approximately zero. These equations may thus be written:

$$\langle Q_j \rangle = Q_j^{QS} + Q_j^{TR} \quad (j = 1, 2). \tag{18}$$

The definition of TR transports in these equations can be used to estimate them. In practice, it is easier to compute TR transports as the difference between subinertial and QS transports. It follows from (16) and (17) that the TR transports must be equal in their absolute value but opposite in sign,  $Q_2^{TR} = -Q_1^{TR}$ . However, the rescaling of the estimated upper layer transport at CS affects also the QS upper layer transport, so that the estimation of the upper and lower layer TR transports at CS are slightly different.

### 3.5. Description of TR and QS transports

The subinertial exchange is achieved in different ways at each section. At ES, the TR transports are practically negligible, having a mean value and standard deviation smaller than 0.1 Sv (Table 3). Therefore, at ES, subinertial transports are almost equal to quasistatic transports and Eq. (18) reads:

$$\langle Q_j \rangle_{(ES)} \simeq Q_{j(ES)}^{QS} \quad (j = 1, 2). \tag{19}$$

On the other hand, TR and QS transports are comparable at CS (Fig. 7, Table 3), as each of them accounts for a significant part of the long-term mean value and the subinertial transports variance (Table 3). Thus, at CS, Eq. (18) still holds:

$$\langle Q_j \rangle_{(CS)} = Q_{j(CS)}^{QS} + Q_{j(CS)}^{TR} \quad (j = 1, 2). \tag{20}$$

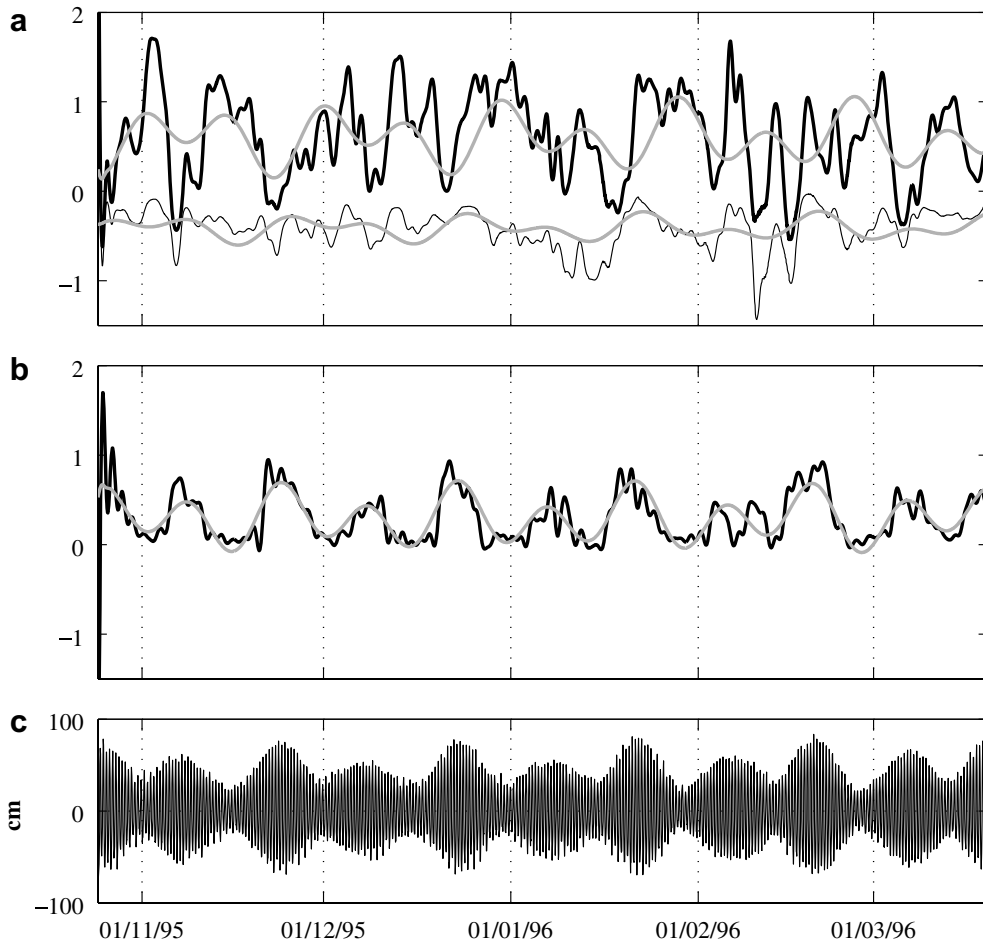


Fig. 7. Time series of (a) quasistatic upper layer  $Q_1^{QS}$  (black, thick line) and quasistatic lower layer transport  $Q_2^{QS}$  (black, thin line) and their  $M_m + M_{sf}$  harmonic fit (gray) at CS; (b) tidally rectified upper layer transport  $Q_1^{TR}$  (black) and its  $M_m + M_{sf}$  harmonic fit (gray) at CS. (d) Tidal signal of the sea level at Tarifa.

The difference, between CS and ES, of the TR transports contribution to the long-term mean is consistent not only with previous observations of García-Lafuente et al. (2000) at ES and Bryden et al. (1994) at CS, but also with recent numerical models (see for example, Sanino et al., 2004). The important fact to be stressed is that, despite the different way in which they are achieved, the subinertial transports are equal, within the estimation error, for each layer, that is,  $\langle Q_j \rangle_{(CS)} = \langle Q_j \rangle_{(ES)}$  (Fig. 6). Then, there is not any internal divergences at subinertial frequencies in the intermediate region between both sections. Such divergences would not have physical explanation in the two layer model we are dealing with. Note that the former equality does not imply that  $Q_{j(CS)}^{QS} = Q_{j(ES)}^{QS}$ . In fact as, in general,  $Q_{j(CS)}^{TR} \neq 0$ , the QS transports must be different from one section to the other for the subinertial transports to be equal.

As TR transports at ES are negligible, the fortnightly and monthly signals of  $Q_{j(ES)}^{QS}$  are approximately equal to that of  $\langle Q_j \rangle_{(ES)}$  given in Section 3.3. On the contrary the TR transports at CS have a dominant fortnightly and monthly variability. They reach absolute values of around 1 Sv on the stronger spring tides, of 0.5 Sv on the moderate ones, and about 0.1 Sv or less on neap tides. In this last case, the approximation (19) also applies at CS, indicating that the subinertial exchange is nearly quasistatic throughout the Strait during neap tides.

QS upper layer transport at CS has important fortnightly (0.25 Sv) and monthly (0.2 Sv) amplitudes, while they are less significant (0.1 Sv) in the QS lower layer transport. As a consequence, the QS upper layer transport at CS may flow toward the Atlantic during specially strong spring tides (see Fig. 6). This reverse

QS transport is enhanced when these intense spring tides eventually coincide with SBT fluctuations toward the Atlantic. This type of inversions are not observed in the QS lower layer transport at CS.

### 3.6. Tidally rectified-quasistatic transport compensation at Camarinal

It is interesting that, in spite of the important fortnightly variability of  $Q_1^{\text{TR}}$  and  $Q_1^{\text{QS}}$ , the fortnightly signal of the subinertial upper layer transport  $\langle Q_1 \rangle = Q_1^{\text{QS}} + Q_1^{\text{TR}}$  is not significant (Table 3, Fig. 7). The explanation is that the fortnightly signals of TR and QS transports have similar amplitudes in the upper layer but they are  $180^\circ$  out of phase, so that they cancel when adding both contributions together. This compensation does not take place in the lower layer, even when both contributions are still  $180^\circ$  out of phase, because the fortnightly signal in the lower layer TR transport has a noticeable stronger amplitude than in the QS transport. Consequently  $\langle Q_2 \rangle$  has a significant fortnightly signal (Table 3).

The mechanism of compensation deserves a more detailed investigation. The variability of the QS transports is due to the subinertial currents (and interface) fluctuations. For a deeper analysis it is convenient to separate the SBT and SBC contributions to the QS transports. This can be achieved by projecting them onto the EOF subinertial modes computed in Section 3.1, according to

$$Q_j^{\text{QS}} = \overline{Q_j^{\text{QS}}} + [Q_j^{\text{QS}}]_{\text{SBT}} + [Q_j^{\text{QS}}]_{\text{SBC}} + r, \quad (21)$$

where  $\overline{Q_j^{\text{QS}}}$  is the QS transport long term mean,  $[Q_j^{\text{QS}}]_{\text{SBT}}$  and  $[Q_j^{\text{QS}}]_{\text{SBC}}$  are the SBT and SBC part of the QS transport, and  $r(t)$  is a residual which is approximately orthogonal to the EOF modes. The residual presumably accounts for little variance, so that we can make the approximation

$$Q_j^{\text{QS}} \simeq \overline{Q_j^{\text{QS}}} + [Q_j^{\text{QS}}]_{\text{SBT}} + [Q_j^{\text{QS}}]_{\text{SBC}}, \quad (22)$$

that accounts for around the 90% of the QS transports variance at CS (66% for SBT, 23% for SBC in the upper layer transport, 80% for SBT, 13% for SBC in the lower layer transport). With the help of (22), Eq. (18) is written as

$$\langle Q_j \rangle \simeq [Q_j^{\text{QS}}]_{\text{SBT}} + [Q_j^{\text{QS}}]_{\text{SBC}} + Q_j^{\text{TR}} \quad (j = 1, 2). \quad (23)$$

The standard deviation of SBC transport fluctuations are  $[Q_1^{\text{QS}}]_{\text{SBC}} \simeq 0.2$  Sv for the upper and  $[Q_2^{\text{QS}}]_{\text{SBC}} \simeq 0.1$  Sv for the lower layer transports, respectively. As already mentioned in Sections 3.1 and 3.3, on neap tides the subinertial current shear between the two layers is enhanced and the interface shallows, while on spring tides the subinertial current shear is reduced and the interface sinks. Both effects combine to enhance  $[Q_1^{\text{QS}}]_{\text{SBC}}$  and to reduce  $[Q_2^{\text{QS}}]_{\text{SBC}}$  fluctuations. This explains the higher variance of SBC transports in the upper layer, despite the fact that SBC velocity fluctuations have a greater variance in the lower than in the upper layer (Fig. 4b).

Fortnightly signal in  $Q_j^{\text{QS}}$  is almost completely due to the baroclinic contribution  $[Q_j^{\text{QS}}]_{\text{SBC}}$ , as the barotropic contribution  $[Q_j^{\text{QS}}]_{\text{SBT}}$  is the flow response to atmospheric forcing which has little fortnightly variability. It follows that the compensation of  $[Q_1^{\text{QS}}]_{\text{SBC}}$  and  $Q_1^{\text{TR}}$  which leads to the cancellation of the fortnightly signal in  $\langle Q_1 \rangle$  actually happens between the baroclinic contribution ( $[Q_1^{\text{QS}}]_{\text{SBC}}$ ) to  $Q_1^{\text{QS}}$  and  $Q_1^{\text{TR}}$  (Fig. 8a). This compensation is not achieved in the lower layer because the fortnightly signal in  $[Q_2^{\text{QS}}]_{\text{SBC}}$  is much smaller than in  $Q_2^{\text{TR}}$  (Fig. 8b). Therefore the subinertial lower layer transport  $\langle Q_j \rangle$  has a significant fortnightly variability, due basically to (and, thus, in-phase with) the signal in  $Q_2^{\text{TR}}$ .

An intriguing feature of fortnightly signal in this analysis is that despite the fact that both  $\langle Q_2 \rangle_{\text{CS}}$  and  $\langle Q_2 \rangle_{\text{ES}}$  have similar fortnightly amplitudes and phases, the signal in the latter is due to the QS term  $Q_{2(\text{ES})}^{\text{QS}}$  while in the former it is due to the TR term  $Q_{2(\text{CS})}^{\text{TR}}$ . Apparently, one should expect similar behavior at both sections, on the basis of continuity reasons. As mentioned above, during neap tides the flow is essentially quasistatic at both sections, fulfilling such continuity arguments. On spring tides, the subinertial flow is still quasistatic at ES but not at CS, where the TR contribution prevails. To interpret this paradox we must think of the region between CS and ES as a reservoir. During spring tides the lower part (lower layer) of the reservoir is smoothly (quasistatically) filled through ES, but at the same time it is emptied at a pulsating rhythm of tidal frequency through CS (TR flow). On average, these outflowing pulses equal the smooth flow through ES, and the reservoir is neither filled nor emptied.

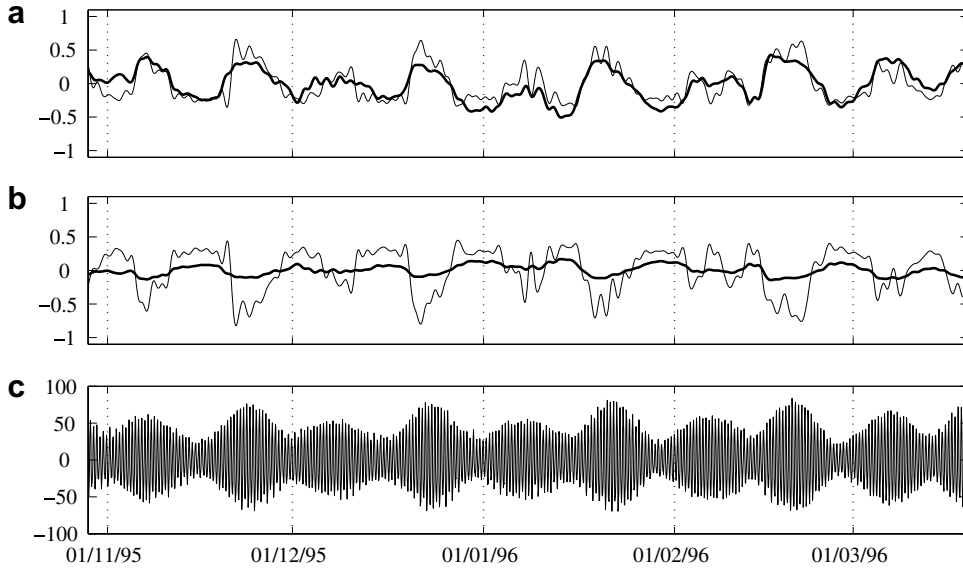


Fig. 8. Camarinal section: (a) Demeaned tidally rectified upper layer transport  $Q_1^{\text{TR}}$  (thin line), and minus SBC upper layer transport,  $-[Q_1^{\text{QS}}]_{\text{SBC}}$  (thick line). (b) Same as in (a) for the lower layer transport. (c) Tidal signal of the sea level at Tarifa.

### 3.7. Tidal mixing and SBC transports

The tidal mixing hypothesis for the origin of the SBC current fluctuations is now explored. Tidal mixing influences the exchange at subinertial time scales by modulating the reduced gravity  $g'$  given by

$$g' = \frac{\rho_2 - \rho_1}{\bar{\rho}} g, \quad (24)$$

where  $\bar{\rho}$  is a reference density, and  $\rho_1$  and  $\rho_2$  are layer-averaged densities. The reduced gravity has a significant fortnightly signal at CS with a phase  $\phi_{M_{\text{sf}}} \simeq 180^\circ$  (Table 3). It means that maximum  $g'$  (maximum density contrast) occurs during neap tides and minimum  $g'$  during spring tides, in good agreement with the hypothesis of tidally driven mixing.

A key prediction of the quasistatic hydraulic theory is that the possible magnitude of the exchanged transports is upper bounded. For the exchange to be in the so called *maximal* state, the flow must be hydraulically controlled at CS but also at Tarifa Narrows (Fig. 1a). If this happens, the exchanged transports reach their maximum allowable value (Armi and Farmer, 1986). Bryden and Kinder (1991) argued that if the exchange is *maximal* in the hydraulic sense, the quasistatic upper and lower layer transports should scale as  $\sqrt{g'}$ .

More precisely, the scaled (baroclinic) transports  $[q_1]_{\text{SBC}}$  and  $[q_2]_{\text{SBC}}$  are

$$[q_1]_{\text{SBC}} \approx -[q_2]_{\text{SBC}} \approx P \cdot \sqrt{g' b_c} \frac{W_c b_c}{2}, \quad (25)$$

where  $b_c \simeq 280$  m and  $W_c \simeq 22.7$  km are the depth of the bottom and the width of the Strait at the surface at CS, and  $P$  is a dimensionless coefficient. Bryden and Kinder (1991) showed that as the historical estimates of the (quasistatic) maximal exchanged flow were refined, the coefficient tends to converge to  $P \simeq 0.14$ .

Based on Eq. (25), we have generated time series of  $[q_1]_{\text{SBC}}$  and  $[q_2]_{\text{SBC}}$  for the upper and lower layer transport. As Eq. (25) is valid for quasistatic exchange, these synthesized transports must be compared with  $[Q_j^{\text{QS}}]_{\text{SBC}}$ , (Section 3.6 and Fig. 10). Fig. 9b shows that  $[q_2]_{\text{SBC}}$  reproduces appropriately the fluctuations of  $[Q_2^{\text{QS}}]_{\text{SBC}}$ . However,  $[q_1]_{\text{SBC}}$  fails in reproducing  $[Q_1^{\text{QS}}]_{\text{SBC}}$  fluctuations (Fig. 9a), as its variance (0.1 Sv rms) is significantly smaller than the variance of  $[Q_1^{\text{QS}}]_{\text{SBC}}$  (0.25 Sv rms).

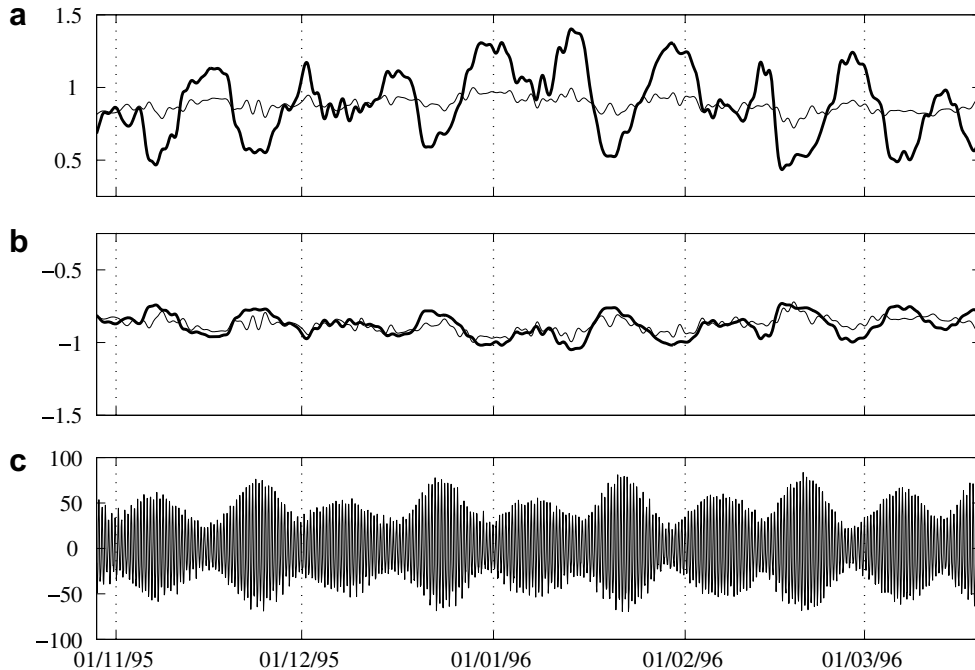


Fig. 9. (a) Reconstruction of the quasistatic upper layer transport fluctuations from Eq. (25), (thin line), and minus SBC upper layer transport fluctuations,  $-[Q_1^{QS}]_{SBC}$  (thick line) at CS. (b) Idem for the lower layer transport. (c) Tidal signal of the sea level at Tarifa.

Thus, the subinertial fluctuations of the transports estimated from the hydraulic theory through Eq. (25) coincide reasonably well with the estimated SBC fluctuations of the quasistatic lower layer transport, but not with those of the quasistatic upper layer transport. Again, the issue of the different variance of the SBC transports in each layer at CS arises. We suspect that the fortnightly variability of the interface depth is possibly responsible for this asymmetry and may be related to the variability of the control condition at CS, in the same manner as the TR transports seem to be. A more complete analysis of this likely relationship would need a detailed analysis of the variability of the hydraulic conditions at CS at diurnal and higher tidal frequencies, which is the subject of a further paper.

### 3.8. Hydraulics implications

An interesting question to be addressed, in the framework of the two-layer hydraulic theory, is to what extent our data are compatible with a permanent control section at CS. The existence of strong tidal currents within the Strait, specially at CS, breaks the quasistatic theory predictions (Helfrich, 1995), and it is generally accepted that the hydraulic control at CS is prone to be lost during a short time interval in each tidal cycle, particularly on spring tides (Armi and Farmer, 1988; Castro et al., 2004). When this happens, an energetic internal bore is released eastwards into the Mediterranean (Izquierdo et al., 2001). However, scarce direct evidence has been provided yet because direct estimation of Froude numbers from the original data are too noisy at tidal frequencies. Here we adopt a different approach. Let us assume the validity of the approximation

$$F_2^2 \simeq 1 \quad (26)$$

as control condition, and rewrite it as

$$[Q_2^2]_H \simeq \frac{g' A_2^3(\eta)}{W_{\text{int}}(\eta)}, \quad (27)$$

where subscript H stands for “hydraulic-based” estimation. The approximation (26) is justified by the fact that the interface is usually sufficiently deep to assume that  $G^2 \simeq F_2^2$ . Only during very short periods on spring tidal

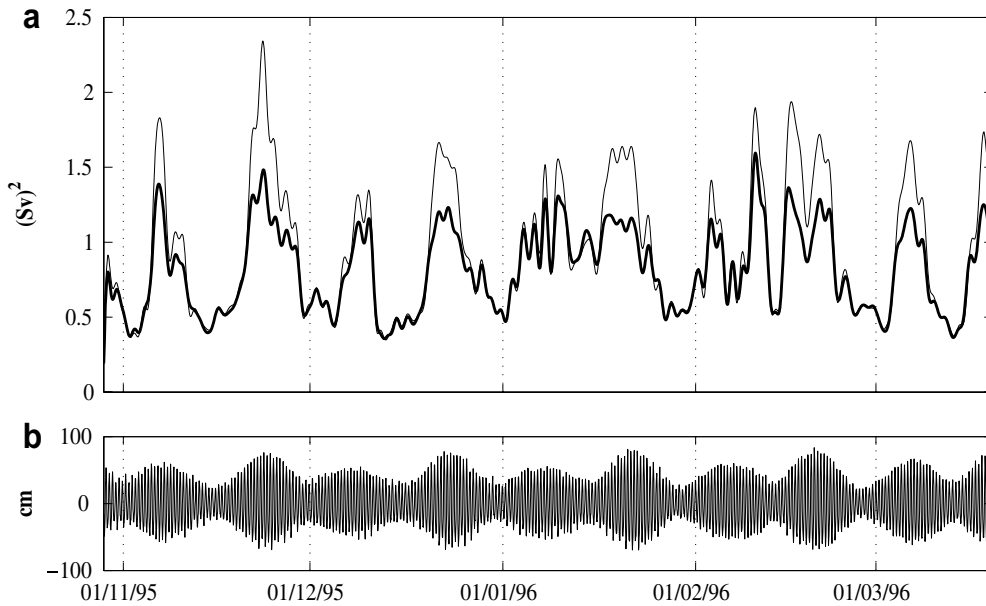


Fig. 10. (a) Reconstruction of the subinertial “hydraulic” lower layer transport  $\langle Q_2 \rangle_H$  from Eq. (28), (thick line), and rms subinertial lower layer transport (thin line) at CS. (b) Tidal signal of the sea level at Tarifa.

cycles the interface shallows enough to make (26) inapplicable. Applying the low-pass filtering operator to Eq. (27) we obtain

$$\langle Q_2 \rangle_H \simeq \left\langle \sqrt{\frac{g' A_2^3(\eta)}{W_{\text{int}}(\eta)}} \right\rangle, \tag{28}$$

$\langle Q_2 \rangle_H$  is interpreted as the subinertial lower layer transport, based in the hydraulic theory, that is compatible with the control condition, provided that the interface depth and reduced gravity estimates at CS are known.

Fig. 10 shows that the time series of  $\langle Q_2 \rangle_H$  and the rms subinertial lower layer transport,  $Q_2^{\text{rms}} = \left\langle \sqrt{Q_2^2} \right\rangle$  are remarkably similar, with a correlation coefficient  $r \simeq 0.97$ . Both time series practically coincide during neap tides and also during weak spring tides. The greatest difference takes place on strong spring tides, when  $Q_2^{\text{rms}}$  is systematically higher than  $\langle Q_2 \rangle_H$ . That means that during strong spring tides the control condition would be lost even if the upper layer contribution to  $G^2$  were not considered. It should be remembered that the fortnightly signal in the lower layer transport is dominated by the TR transports. This fact suggests that the mechanism that triggers TR transports during spring tides is related to the lost of the hydraulic control at CS.

#### 4. Conclusions

In this paper the fortnightly and monthly variability of the exchange through the Strait of Gibraltar has been studied from a five months mooring time series simultaneously acquired at two sections of the Strait of Gibraltar, that is, the Camarinal and East sections.

To this aim we have estimated time series of the subinertial exchanged transports,  $\langle Q_1 \rangle$  and  $\langle Q_2 \rangle$ , and analyzed them at these frequencies. A significant monthly signal is observed in the upper layer transport, but not in the lower layer transport, which exhibits a significant fortnightly signal. The minimum (maximum absolute value) lower layer transport takes place, approximately, on spring tides. Consequently, the net transport shows a combination of both signals with maximum value (toward the Mediterranean) on neap tides, with a certain monthly inequality. A significant fortnightly and monthly variability of interface depth is also

observed at CS: it is deeper on neap and shallower on spring tides. At ES these signals in the interface depth are less pronounced.

The subinertial exchanged transports have been separated into tidally rectified (TR) and quasistatic (QS) parts. QS transports are computed from subinertial interface depth and currents fluctuations or, in other words, the time series of interface depth and currents are low-pass filtered prior to QS transports estimate. TR transports, that arise from positive correlations of currents and interface depth at tidal frequencies, are computed as the difference of subinertial and quasistatic transports.

TR transports are not significant at ES, but they are important at CS, contributing both to the long-term mean and to the subinertial fluctuations of the exchanged transports at this section. They are linked to the fortnightly and monthly cycles: they are of little importance (of the order of 0.1 Sv) on neap tides but of great amplitude (around 1 Sv) on spring tides.

The fortnightly signals of QS and TR transports at CS are in phase opposition, so that they tend to cancel one another. This compensation is quite efficient in the upper layer transport, removing the fortnightly signal in the total upper layer subinertial transport  $\langle Q_1 \rangle$ , but not so efficient in the lower layer transport, in which TR transports provides a clear fortnightly signal to the lower layer subinertial transport  $\langle Q_2 \rangle$ .

The difference in the character of the fortnightly and monthly signals of upper and lower layer transport is a consequence of the asymmetry in the quasistatic transports at CS, whose variance is higher for the upper layer transport than for the lower layer transport.

Finally, it has been found that the time series of the estimated lower layer transports is strongly compatible with existence of hydraulic control at CS on neap and on moderate spring tides. During strong spring tides the estimated subinertial lower layer transport exceeds the predictions of the hydraulic theory for controlled flow, confirming that control is lost in these periods.

## Acknowledgments

This research has been partially supported by the CICYT through contracts REN2001-2733-C02-01 and REN2003-01608.

## References

- Armi, L., Farmer, D.M., 1986. Maximal two layer exchange through a contraction with barotropic net flow. *Journal of Fluid Mechanics* 164, 27–51.
- Armi, L., Farmer, D.M., 1988. The flow of Mediterranean water through the Strait of Gibraltar; the flow of Atlantic water through the Strait of Gibraltar. *Progress in Oceanography* 21, 1–105.
- Baschek, B., Send, U., Lafuente, J.G., Candela, J., 2001. Transport estimates in the Strait of Gibraltar with a tidal inverse model. *Journal of Geophysical Research* 106, 31033–31044.
- Bormans, M., Garrett, C., 1989. The effects of nonrectangular cross section, friction and barotropic fluctuations on the exchange through the Strait of Gibraltar. *Journal of Physical Oceanography* 19, 1543–1557.
- Bray, N.A., Ochoa, J., Kinder, T.H., 1995. The role of the interface in exchange through the Strait of Gibraltar. *Journal of Geophysical Research* 100, 10755–10776.
- Bruno, M., Mañanes, R., Alonso, J.J., Izquierdo, A., Tejedor, L., Kagan, B.A., 1999. Vertical Structure of the semidiurnal tidal currents at Camarinal Sill, the Strait of Gibraltar. *Oceanologica Acta* 23, 15–24.
- Bruno, M., Alonso, J.J., Cózar, A., Vidal, J., Ruiz Cañavate, A., Echevarría, F., Ruiz, J., 2002. The boiling-water phenomena at Camarinal Sill, the Strait of Gibraltar. *Deep-Sea Research* 49, 4097–4113.
- Bryden, H.L., Kinder, T.H., 1991. Steady two layer exchange through the Strait of Gibraltar. *Deep-Sea Research* 38, S445–S463.
- Bryden, H.L., Stommel, H., 1984. Limiting processes that determine basic features of the circulation in the Mediterranean Sea. *Oceanologica Acta* 7, 289–296.
- Bryden, H.L., Candela, J., Kinder, T.H., 1994. Exchange through the Strait of Gibraltar. *Progress in Oceanography* 33, 201–248.
- Candela, J., 2001. Mediterranean water and global circulation. In: Gould, Siedler, Church (Eds.), *Ocean Circulation and Climate: Observing and Modeling the Global Ocean*. Academic Press, pp. 419–429.
- Candela, J., Winant, C., Bryden, H.L., 1989. Meteorologically forced subinertial flows through the Strait of Gibraltar. *Journal of Geophysical Research* 94, 12667–12674.
- Candela, J., Winant, C., Ruiz, A., 1990. Tides in the Strait of Gibraltar. *Journal of Geophysical Research* 95, 7313–7335.
- Castro, M.J., Garcia-Rodriguez, J.A., Gonzalez-Vida, J.M., Macias, J., Pares, C., Vazquez Cendon, M., 2004. Numerical simulation of two-layer Shallow Water flows through channels with irregular geometry. *Journal of Computational Physics* 195 (1), 591–626.

- Crepon, M., 1965. Influence de la pression atmospherique sur le niveau moyen de la Mediterranée Occidentale et sur le flux á travers le détroit de Gibraltar. *Cahiers Orstom Oceanographie* 1 (7), 15–32.
- Delgado, J., García-Lafuente, J., Vargas, J.M., 2001. A simple model for submaximal exchange through the Strait of Gibraltar. *Scientia Marina* 65 (4), 313–322.
- Echevarria, F., García-Lafuente, J., Bruno, M., Gorsky, G., Goutxe, M., Gonzalez, N., Garcia, C., Gomez, F., Vargas, J.M., Picheral, M., Stribye, L., Varela, M., Alonso, J.J., Reul, A., Cozar, A., Prieto, L., Sarhan, T., Plaza, F., Jimenez-Gomez, F., 2002. Physical-biological coupling in the Strait of Gibraltar. *Deep-Sea Research II* 49, 4115–4130.
- Farmer, D.M., Armi, L., 1986. Maximal two layer exchange over a sill and through the combination of a sill and a contraction with barotropic flow. *Journal of Fluid Mechanics* 164, 53–76.
- García-Lafuente, J., Vargas, J.M., 2003. Recent observations of the exchanged flows through the Strait of Gibraltar and their fluctuations at different time scales. In: *Recent Research Development in Geophysics. Research Signpost*, 37/661 (2), Fort P.O., Trivandrum 695 023, Kerala, India, pp. 73–84.
- García-Lafuente, J., Vargas, J.M., Plaza, F., Sarhan, T., Candela, J., Bascheck, B., 2000. Tide at the eastern section of the Strait of Gibraltar. *Journal of Geophysical Research* 105, 14197–14213.
- García-Lafuente, J., Alvarez-Fanjul, E., Vargas, J.M., Ratsimandresy, A.W., 2002a. Subinertial variability through the Strait of Gibraltar. *Journal of Geophysical Research* 107, 32.1–32.9.
- García-Lafuente, J., Delgado, J., Vargas, J.M., Vargas, M., Plaza, F., Sarhan, T., 2002b. Low-frequency variability of the exchanged flows through the Strait of Gibraltar during CANIGO. *Deep-Sea Research I* 49, 4051–4067.
- Garrett, C.J., Akerley, J., Thompson, K.R., 1989. Low-frequency fluctuations in the Strait of Gibraltar from MEDALPEX sea level data. *Journal of Physical Oceanography* 19, 1682–1696.
- Helfrich, K.R., 1995. Time-dependent two-layer hydraulic exchange flows. *Journal of Physical Oceanography* 25, 359–373.
- Hibiya, T., Leblond, P.H., 1993. The control of fjord circulation by fortnightly modulation and tidal mixing processes. *Journal of Physical Oceanography* 23, 2042–2052.
- Hibiya, T., Ogasawara, M., Niwa, Y., 1998. A numerical study of the fortnightly modulation of basin-ocean water exchange across a tidal mixing zone. *Journal of Physical Oceanography* 28, 1224–1235.
- Hogg, A., Ivey, G., Winters, K., 2001. Hydraulic and mixing in controlled exchange flows. *Journal of Geophysical Research* 106, 959–972.
- Izquierdo, A., Tejedor, L., Sein, D.V., Backhaus, J.O., Brandt, P., Rubino, A., Kagan, B.A., 2001. Control variability and internal bore evolution in the Strait of Gibraltar: a 2-D two layer model study. *Estuarine, Coastal and Shelf Science* 53, 637–651.
- Kinder, T.H., Bryden, H.L., 1987. The 1985–1986 Gibraltar experiment: data collection and preliminary results. *EOS* 68, 786–787, 793–795.
- Kinder, T.H., Bryden, H.L., 1988. Gibraltar experiment: summary of the field program and initial results of the Gibraltar Experiment. WHOI-88-30, Woods Hole Oceanographic Institution Technical Report.
- Lacombe, H., Richez, C., 1982. The regime of the Strait of Gibraltar. In: Nihoul, J.J. (Ed.), *Hydrodynamics of Semi-Enclosed Seas*. Elsevier, Amsterdam, pp. 13–73.
- La Violette, P.E., Arnone, R.A., 1988. A tide-generated internal waveform in the western approaches to the Strait of Gibraltar. *Journal of Geophysical Research* 93, 15653–15667.
- La Violette, P.E., Lacombe, H., 1988. Tidal induced pulses in the flow through the Strait of Gibraltar. *Oceanologica Acta*, SP (9), 13–27.
- Sanino, G., Bargagli, A., Artale, V., 2004. Numerical modelling of the semidiurnal tidal exchange through the Strait of Gibraltar. *Journal of Geophysical Research* 109, C05011. doi:10.1029/2003JC002057.
- Tsimplis, M.N., Bryden, H.L., 2000. Estimation of the transports through the Strait of Gibraltar. *Deep-Sea Research I* 47, 2219–2242.
- Vargas, J.M., 2004. Fluctuaciones subinerciales y estado hidráulico del intercambio a través del Estrecho de Gibraltar. Ph.D. thesis, Universidad de Sevilla, Spain. Available from: <[http://fondosdigitales.us.es/thesis/thesis\\_view?oid=407](http://fondosdigitales.us.es/thesis/thesis_view?oid=407)>.
- Wesson, J., Gregg, M.C., 1994. Mixing at Camarinal Sill in the Strait of Gibraltar. *Journal of Geophysical Research* 99, 9847–9878.